Thin-layer boilover of large-scale diesel pool fires at sub-atmospheric pressure

Jinlong Zhao[a,b], Qingyuan Zhang[a], Zhenqi Hu[a], Rongxue Kang[a,b*], Grunde Jomaas[c,d], Rui Yang[e]

a. School of Emergency Management & Safety Engineering, China University of Mining & Technology (Beijing), Beijing, China

b. China Academy of Safety Science and Technology, Beijing, China

c. FRISSBE, Slovenian National Building and Civil Engineering Institute (ZAG), Ljubljana, Slovenia

d. FAMNIT, University of Primorska, Koper, Slovenia

e. Institute of Public Safety Research, Department of Engineering Physics, Tsinghua University, Beijing, China

Abstract

As thin-layer burning of fuels on water are often followed by thin-layer boilover fires, particularly during the firefighting process, an experimental and numerical study was undertaken to address key aspects of such fires, especially in plateau areas (i.e., sub-atmospheric pressure). In the thin-layer boilover experiments at sub-atmospheric pressure (69 kPa), diesel was used as the fuel in five circular steel trays (ranging from 0.4 m to 1.2 m in diameter) and a square steel tray (side length of 2.5 m). The burning process, and especially the continuous boilover stage, was presented and the corresponding boilover intensity, time to boilover onset and boilover time interval were measured and analyzed. The results show that the flame height increased sharply

at the initial boilover, while this increasing range gradually became weak for the subsequent boilovers. The initial boilover intensity showed a linear dependency on the fuel layer thickness at the time of boilover, and the slope of the boilover intensity line decreased with increasing pan area. Eventually, the effect of pan area on boilover intensity became limit. Moreover, a predictive model for the boilover intensity was established based on dimensionless analysis. The initial boilover onset time under the sub-atmospheric pressure was delayed compared with that under atmospheric pressure. The corresponding predictive correlation (for 69 kPa) with different diameter and fuel thickness was developed based on the one-dimension two-layer conduction model. In the end, the boilover time interval decreased with the boilover times, closing to uninterrupted boilover eventually. This work enriches the thin-layer boilover behavior experimental data at sub-atmospheric pressure and provides guidance for the fuel storage safety.

Keywords： thin-layer boilover; boilover intensity; time to boilover onset; boilover time interval; sub-atmospheric fires

1. Introduction

In recent years, due to the vast development space and outstanding resource advantages in western China, the eastern chemical plants are accelerating the transfer to the western regions. Liquid fuel fire accidents occur from time to time in these harsh environments at high altitude, which pose a great threat to liquid fuel security. In the process of firefighting, firefighters usually use a large amount of water, resulting in a thin water layer beneath the liquid fuel. The liquid fuel burning on the

water can result in boilover, causing some serious consequences. For example, in 2014, a 5000 m^3 crude oil storage tank fire accident occurred in a chemical company in Aksu, Xinjiang Province (altitude: 1150 m), in which crude oil leaked and burned [1]. During the firefighting process, the crude oil floated on the water layer and thin-layer boilover occurred. Numerous boilovers followed the initial boilover and caused difficulty to the firefighting.

Several aspects related to the altitude are adding to the already large challenges of such fires. First, the burning characteristics of liquid fuel are changed at sub-atmospheric pressure [2]. Second, the boiling points of liquid fuel and water will be reduced [3]. As a result, the boilover behaviors at sub-atmospheric pressure are different from those under atmospheric pressure. Therefore, it is of interest to study the boilover behaviors of liquid fuel at sub-atmospheric pressure conditions to ensure the liquid fuel security in plateau areas.

The boilover phenomenon has been investigated experimentally in the past and much attention has been paid to the boilover behaviors. Fan et al. [4] carried out small-scale boilover burning experiments on a water surface and analyzed the burning process. According to the flame height and flame shape, they divided the burning process into three stages: quasi-steady stage, boilover premonitory stage and boilover stage. Koseki et al. [5] performed some larger scale (D: 0.3 m - 2.7 m) boilover experiments using Arabian light crude oil and measured the mass burning rate and flame radiation values. They found that burning rate and flame radiation increased dramatically and proposed the concept of boilover intensity, which is defined as the

ratio of the mass burning rate at the boilover stage to the mass burning rate at the stable stage. Ferrero et al. [6] conducted a series of thin-layer boilover fire experiments with different diameters (D: 1.5 m - 5 m) and initial fuel layer thicknesses (h_0: 10 mm - 30 mm). They focused on the initial boilover intensity and developed a predictive expression ($I_{b,max} = -25.3 + 262.1\exp(-\frac{D}{2.37})$). They also found that the limiting factor for initial boilover intensity was the residual fuel at the boilover onset. Kong et al. [7] experimentally studied the boilover fires at different scales (D: 0.1 m - 0.2 m) and initial fuel thicknesses (h_0: 5 mm - 15 mm) using crude oil and recorded the time to boilover onset. They found that the time to boilover onset showed a linear dependency on the initial fuel layer thickness and decreased with the increase of pan diameter. Chen et al. [8] carried out some small-scale (D: 15 cm - 18 cm) boilover experiments using diesel and kerosene with the initial fuel layer thickness of 7.5 mm in Hefei (100.8 kPa) and Lhasa (64 kPa), respectively. They compared the boilover onset time and initial boilover intensity at two places and obtained that the pressure had a negative correlation with boilover onset time and a positive correlation with initial boilover intensity. Ding [3] conducted a series of thin-layer burning experiments on a water layer with different diameters (D: 15 cm - 18 cm) and pressures (54 kPa - 101 kPa) and focused on the effect of pressure on the time to boilover onset. He found that for the same pan diameter, the lower the ambient pressure was, the later the initial boilover occurred. He also proposed a simplified expression for the time to boilover onset based on the ambient pressure ($\frac{1}{t(P)} = c_1P^2 + c_2$). Lin [9] performed thin-layer boilover burning experiments (D: 15 cm - 40

cm; h_0: 10 mm) for three different pressures (64 kPa, 76 kPa and 101 kPa). He found that with the increase of air pressure, the residual fuel layer at the boilover onset and the corresponding initial boilover intensity increased.

The above studies, mainly focusing on the boilover behaviors under atmospheric pressure, indicate that the fuel layer thickness and pan diameter both significantly impact boilover behaviors. There are also some studies on boilover behaviors at sub-atmospheric pressure. However, it appears that available literature for studies at sub-atmospheric pressure are based on experiments at a relatively small-scale, thus rendering the experimental data of large-scale boilover fires, which are more relevant for actual fires, to be limited. Therefore, the boilover behaviors at sub-atmospheric pressure are still unclear and need further investigating. Moreover, the initial boilover has been widely studied in the previous studies, while the boilover behaviors of the subsequent multiple boilovers after initial boilover, which is of importance to fire rescue, have received little attention.

Some scholars have also been committed to the investigate in boilover mechanism. Arai et al. [10] conducted a series of small-scale (D: 4.8 cm - 20.3 cm) boilover experiments and studied the burning behaviors using 16 different single and multicomponent fuels. They proposed that boilover occurred only when the boiling point of fuel was higher than that of water. Broeckmann et al. [11] carried out some boilover experiments on a water layer with different diameter pans (D: 0.19 m - 1.9 m) and analyzed the heat transfer process of thin-layer boilover. It was found that a boiling layer with stable temperature was formed at the fuel surface during burning

process and an essential condition for boilover occurrence is the temperature at interface reaching water boiling point. Twardus and Brzustowski [12] first developed a simple one-dimensional model to describe the burning process of boilover fire with a heat loss from fuel towards the water layer. Subsequently, this developed model was modified by incorporating the radiative absorption in the fuel layer [13]. Alramadhan et al. [14] developed a more realistic model by using existing experimental data. This model incorporated radiative feedback and the effects of turbulent buoyant motion. Based on the experimental data of Arai et al. [10], Inamura et al. [15] used the liquid layer temperature and flame radiation to establish the one-dimensional transient model. This model took into account the conduction and absorption of radiation through the fuel layer to predict the time to boilover onset. Garo et al. [16] performed small scale (D: 15 cm - 50 cm) experiments on water using heating oil and crude oil with different initial fuel layer thicknesses (h_0: 2 mm - 20 mm). One-dimensional models of single layer and double layers were established and the temperature distribution inside the liquid layer was predicted. The above studies show that the occurrence of boilover is closely related to the heat transfer in liquid layer. The influence of reduced ambient pressure on the heat transfer in fuel layer and boilover occurrence is ignored and merits further study.

The following describes experimental research on the boilover behaviors of large-scale thin-layer diesel burning at sub-atmospheric pressure. The boilover characteristics including boilover intensity, time to boilover onset and boilover time interval were analyzed in detail. Meanwhile, the influence of initial fuel layer

thickness and pan diameter on above-mentioned parameters were also investigated. The corresponding predictions of boilover intensity and time to boilover onset were established through novel expressions.

2. Experimental setup and theoretical model

2.1. Experimental setup

The detail experimental setup and the measurement methods have been shown in a previous publication [17] and they are therefore only described briefly at here. In the experiments, two types fuel pans made of stainless steel (3 mm thick) were used to resemble the fire pools. One type is circular with diameters of 40, 60, 80, 100 and 120 cm, with the same side wall height of 20 cm. The other type is square with a side length (L) of 2.5 m (equivalent diameter of 2.8 m, $D' = 2L/\sqrt{\pi}$). Water was added beneath the fuel layer for all tests until the water layer thickness achieved 10 cm. Different initial fuel layer thicknesses were used, ranging from 3 to 25 mm. The liquid temperature profiles during the burning were measured with an array of seven K-type thermocouples (maximum: 1200 K; bead diameter: 1 mm) labeled as T1-T7 from the bottom to the top along the centerline inside the pan. The vertical gap between two neighboring thermocouples was 5 mm, in which the first thermocouple T1 was 9 cm above the pan bottom.

Diesel fuel with a purity of more than 99 % was selected for all tests and the main physical properties were shown in Table 1.

Table 1. Thermal properties of the diesel fuel

Properties	Value

Flash point (℃)	65
Density (kg/m^3)	835
Latent heat of evaporation (kJ/kg)	250
Heat of combustion (MJ/kg)	42

All experiments were performed in an outdoor environment in the Qinghai Province (atmospheric pressure: 69 kPa, which was measured locally using a barometer). A windproof net was installed around the experimental site to reduce the impact of environmental winds. The wind speed near the fuel pan was less than 1 m/s during the experiments, in which the influence of wind can be ignored. A total of 33 tests were carried out and the specific conditions of each test are shown in Table 2. All tests were repeated three times to guarantee the reliability.

Table 2. Specification of the Test Conditions

No.	Pan diameter D (cm)	Initial fuel layer thickness h_0 (mm)	No.	Pan diameter D (cm)	Initial fuel layer thickness h_0 (mm)
1	40	3	18	80	25
2	40	5	19	100	3
3	40	10	20	100	5
4	40	15	21	100	10
5	40	20	22	100	15
6	40	25	23	100	20
7	60	3	24	100	25
8	60	5	25	120	3

9	60	10	26	120	5
10	60	15	27	120	10
11	60	20	28	120	15
12	60	25	29	120	20
13	80	3	30	280	3
14	80	5	31	280	5
15	80	10	32	280	10
16	80	15	33	280	15
17	80	20			

2.2. Theoretical model

The heat release rate from a pool fire has been extensively studied by scholars. It can be expressed as [13,18]:

$$\dot{Q} = \rho_\infty C_p (T_\infty g (T_f - T_\infty))^{1/2} D^{5/2} \quad (1)$$

where ρ_∞ is the ambient air density, kg/m^3; C_p is the specific heat at constant pressure, kJ/(kg·K); T_f and T_∞ represent the flame temperature and the ambient temperature respectively, K; g is the acceleration of gravity, m/s^2.

The heat feedback from flame to fuel surface is a fraction of the total heat release. The proportional coefficient is found independent of the pan diameter [19]. Thus, the heat flux feedback from the flame (per unit) reaching the fuel surface ($\dot{q}_s''$) can be expressed as:

$$\dot{q}_s'' = (\frac{4\chi}{\pi})\rho_\infty C_p (T_\infty g\big(T_f - T_\infty\big) D)^{1/2} \quad (2)$$

where χ is the radiative fraction of the radiation feedback to the pool surface.

For thin-layer burning on a water layer, heat conduction is the main heat transfer mechanism in liquid layer, as shown in Fig. 1, assuming that no convection inside the fuel layer occurs. During the burning process, the liquid layer decreases in depth at a regression rate *r(t)*. the radiative heat flux is fully absorbed at the fuel surface $y=y_s(t)$, where the energy balance is:

$$\dot{q}_s'' = L_v \rho_F r(t) + \dot{q}_c'' \tag{3}$$

where the heat conducted into the fuel layer ($\dot{q}_c''$) can be expressed as:

$$\dot{q}_c'' = -\lambda_F \frac{\partial T}{\partial y}\Big|_{y=y_s(t)} \tag{4}$$

where L_v is the the latent heat of vaporization, kJ/kg; ρ_F is the fuel density, kg/m^3; λ_F is the thermal conductivity of fuel; $y_s(t)$ represents the location of the fuel surface at a specific time.

The thermal diffusivity of water is significantly bigger than that of the liquid fuel. The propagation velocity of thermal wave in water layer and fuel layer is obviously different [16]. One-dimensional two-layer conduction model is proposed to more accurately describe the heat transfer process of boilover pool fire.

For fuel layer:

$$\frac{\partial^2 T}{\partial y^2} = \frac{1}{a_F}\frac{\partial T}{\partial t} \tag{5}$$

For the water layer:

$$\frac{\partial^2 T}{\partial y^2} = \frac{1}{a_W}\frac{\partial T}{\partial t} \tag{6}$$

With initial condition at

$$t=0,\ T=T_\infty \tag{7a}$$

and boundary conditions

$$T = T_S,\ y = y_s(t), \tag{7b}$$

$$y = 0,\ -\lambda_F \frac{\partial T}{\partial y}\Big|_{y=0^-} = -\lambda_w \frac{\partial T}{\partial y}\Big|_{y=0^+} \tag{7c}$$

$$y \to \infty,\ T = T_\infty. \tag{7d}$$

where α_F and α_W are the thermal diffusivity of fuel and water, respectively; λ_w is the thermal conductivity of water.

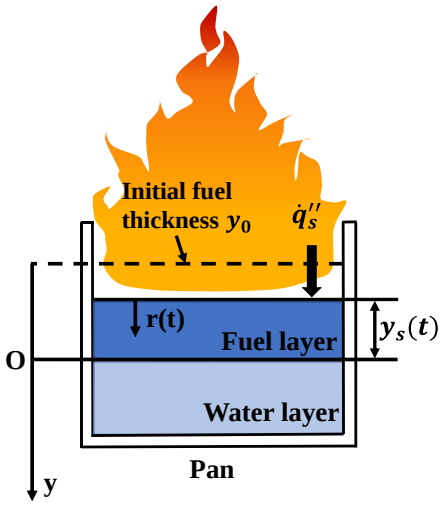

Fig. 1. Coordinate system for liquid fuel pool fires supported on a water layer.

Garo et al. [16] obtained the equivalent thermal diffusivity by matching the thermal penetration distance through a two-layer bed with thermal diffusivities α_F and α_W and the thermal penetration distance in one single layer of thermal diffusivity α_{FW}.

$$\alpha_{FW} = \frac{r y_0}{\alpha_F} \left(\sqrt{\alpha_W} + \sqrt{\alpha_F}\right)^2 \tag{8}$$

where y_0 is the initial fuel layer thickness; r is the regression rate, which is assumed to be constant.

The two-layer conduction model can be simplified into a single layer model. Combined with Eq. (3), the expression for the average regression rate is obtained [20]:

$$r = \frac{1}{L_v \rho_F}\left[\left(\frac{4\chi}{\pi}\right)\rho_\infty C_p \left(T_\infty g\left(T_f - T_\infty\right)\right)^{\frac{1}{2}} D^{\frac{1}{2}} - \frac{\lambda_F \alpha_F (T_S - T_\infty)}{y_0\left(\sqrt{\alpha_W}+\sqrt{\alpha_F}\right)^2}\right] \quad (9)$$

3. Results and discussion

3.1. Burning process and boilover behaviors

Figure 2 shows the flame evolution of thin-layer diesel boilover fire during the whole burning process at sub-atmospheric pressure. It is consistent with the burning process at atmospheric pressure [21], which can be divided into four stages: (1) initial development stage; (2) steady burning stage; (3) continuous boilover stage; (4) decay stage. It is worth noting that the boilover occurred before the burning reached the steady burning stage for tests with an initial fuel layer thickness of 3 mm. For the continuous boilover stage, the flame expanded rapidly, and the flame height increased sharply, accompanied by a loud sound. A large amount of fuel droplets was ejected outside the fuel pan. After a short period of boilover, the flame height decreased significantly, followed by a weak burning. As the burning progressed, the flame height gradually increased again. A second boilover occurred, but with a smaller flame height compared with that at the initial boilover. Subsequently, multiple boilovers occurred and the flame height at boilover decreased gradually until the flame was extinguished, accompanied by the reduction of boilover time interval.

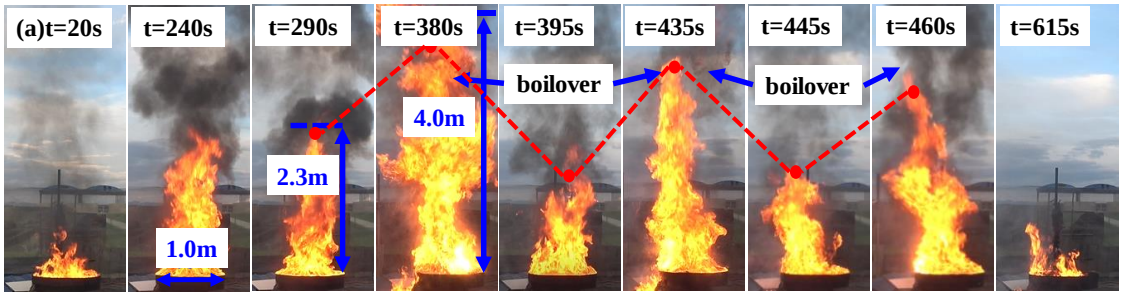

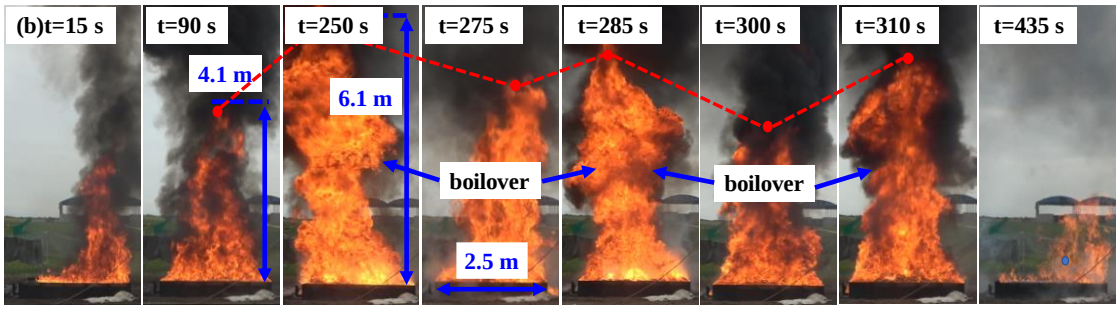

Fig. 2. The evolution of the flame during the boilover fire: a) D = 100 cm, h_0 = 15 mm; b) D = 280 cm, h_0 = 15 mm.

The occurrence of continuous boilover is closely associated with the heat transfer in the liquid layer. Figure 3 shows the schematic of the temperature variation in the fuel layer and the heat transfer in liquid layer, respectively. It can be observed in Fig. 3(b) that a boiling layer was formed at the upper fuel layer (about 3 mm) during steady burning stage [22]. Meanwhile, a large quantity of water vapor bubbles was continuously generated at the fuel/water interface under the effect of heat diffusion. When boilover occurred, these bubbles carried the fuel from pan to the flame, resulting in violent burning. The convective heat transfer between water layer and fuel layer was also enhanced, which destroyed the boiling layer. As a result, the temperature in the fuel layer decreased sharply, as shown in Fig. 3(a), and the burning became weak. Subsequently, the temperature of fuel layer continued to increase again by absorbing the radiative heat feedback from the flame to the fuel surface until a second boilover occurred. This process was repeated many times until the flame extinguished.

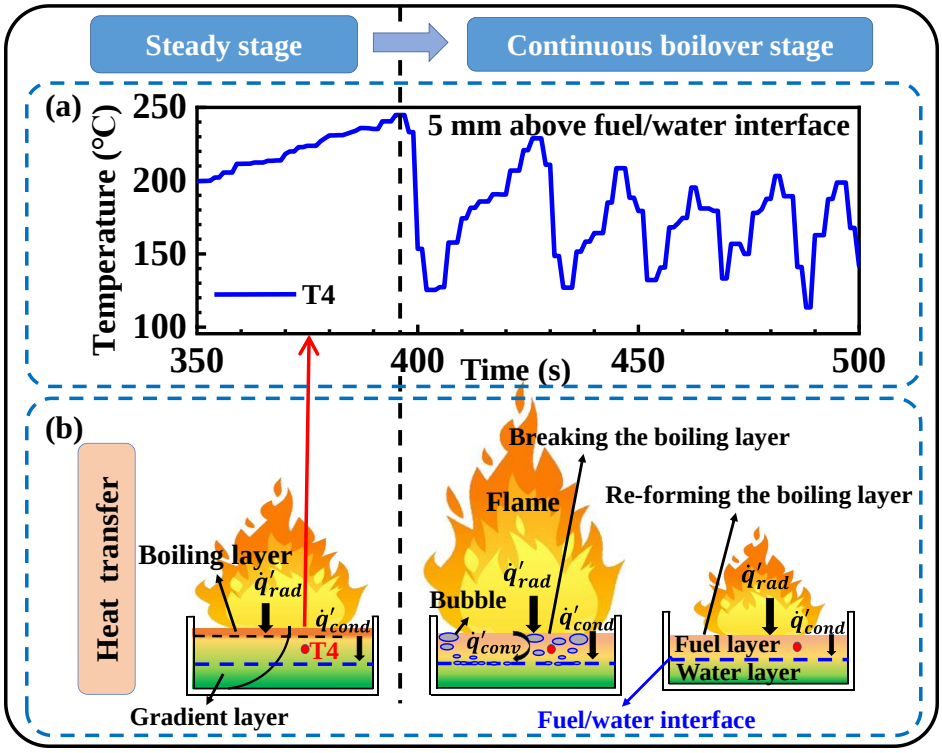

Fig. 3. Schematic and plot of a) temperature variation in the fuel layer (D = 100 cm, h_0 = 15 mm); b) heat transfer in the liquid layer.

In addition, compared with Fig. 2(a) and Fig. 2(b), it was found that the increasing range of flame height before and after boilover decreased with the increasing pan diameter, which indicated the decrease of boilover intensity. This was mainly due to that, for large-scale pool fires, the mass burning rate was large and fuel was consumed fast, leading to a thin residual fuel layer thickness at boilover onset. Thus, the pressure at the fuel/water interface was low and few bubbles were generated. Meanwhile, it was observed in the experiments that for large scale burning, the initial boilover occurred earlier and the boilover time interval was shortened.

3.2. Boilover intensity

Boilover intensity is an important parameter to characterize the burning characteristics of liquid fuel boilover fires [6]. Koseki [5] proposed an expression for

boilover intensity based on the mass burning rate as follows:

$$I_{b,a} = \frac{\dot{m}_{b,a}}{\dot{m}_s} \tag{10}$$

where $\dot{m}_{b,a}$ is the average mass burning rate at the boilover stage, g/(m^2·s), whereas $\dot{m}_s$ is the mass burning rate at the steady stage, g/(m^2·s).

In addition, the boilover intensity can be defined based on the flame enlargement. In the experiments, flame images were captured using a CCD camera with a frequency of 25 fps, and flame contour recognition algorithm was used to determine the flame height according to proportion [23-24]. Based on the flame height, the boilover intensity can be calculated by the following equation:

$$I_{b,a} = \frac{L_{b,a}}{L_s} \tag{11}$$

where $L_{b,a}$ is the average flame height at the boilover stage, m; L_S is the average flame height at steady stage, m. Figure 4 presents the evolution of boilover intensity at sub-atmospheric pressure with the burning time based on mass burning rate and flame height, respectively.

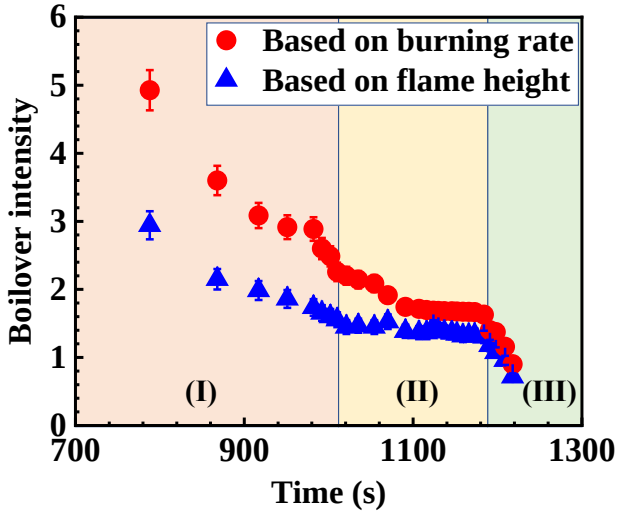

Fig. 4. The boilover intensity evolution versus burning time (D = 40 cm, h_0 = 20 mm).

As shown in Fig. 4, the initial boilover intensity is the most intense, and then

boilover intensity reduces significantly at the next few boilovers. As the burning progresses, the boilover intensity tend to be almost constant with short boilover time interval. After multiple boilovers, the remaining fuel amount is unable to support high-strength boilover followed by several weak boilovers. According to the variation of boilover intensity with burning time, the diesel boilover process can be further divided into: (I) strong boilover period, (II) uninterrupted boilover period and (III) weak boilover period. Moreover, it can be observed in Fig. 4 that the boilover intensity based on mass burning rate is significantly greater than that based on flame height. This is mainly due to that the calculated mass burning rate is obtained based on the mass loss of the fuel in the pan. However, a large number of fuel droplets are thrown out of the fuel pan when boilover occurs, which is not completely involved in burning [14]. In the subsequent analysis of this paper, the boilover intensity is calculated based on flame height.

3.2.1. Boilover intensity with fuel layer thickness

The effect of fuel layer thickness on boilover intensity is further analyzed. Figure 5 shows the boilover intensity of diesel at different residual fuel layer thicknesses during the strong boilover period at sub-atmospheric pressure.

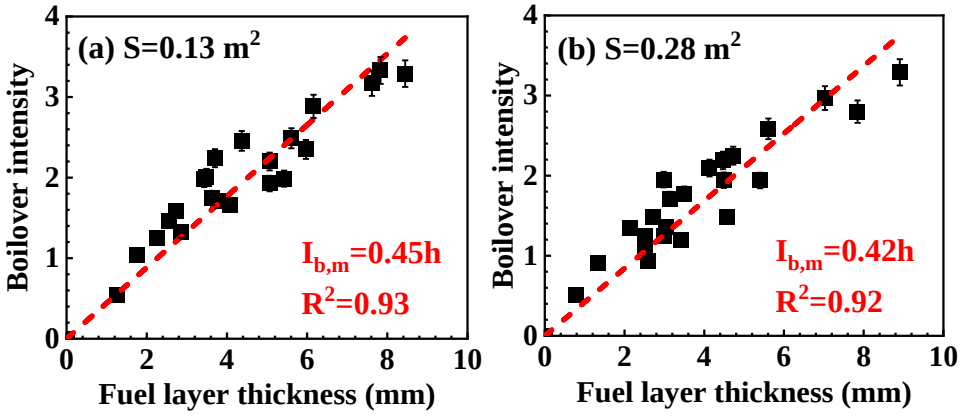

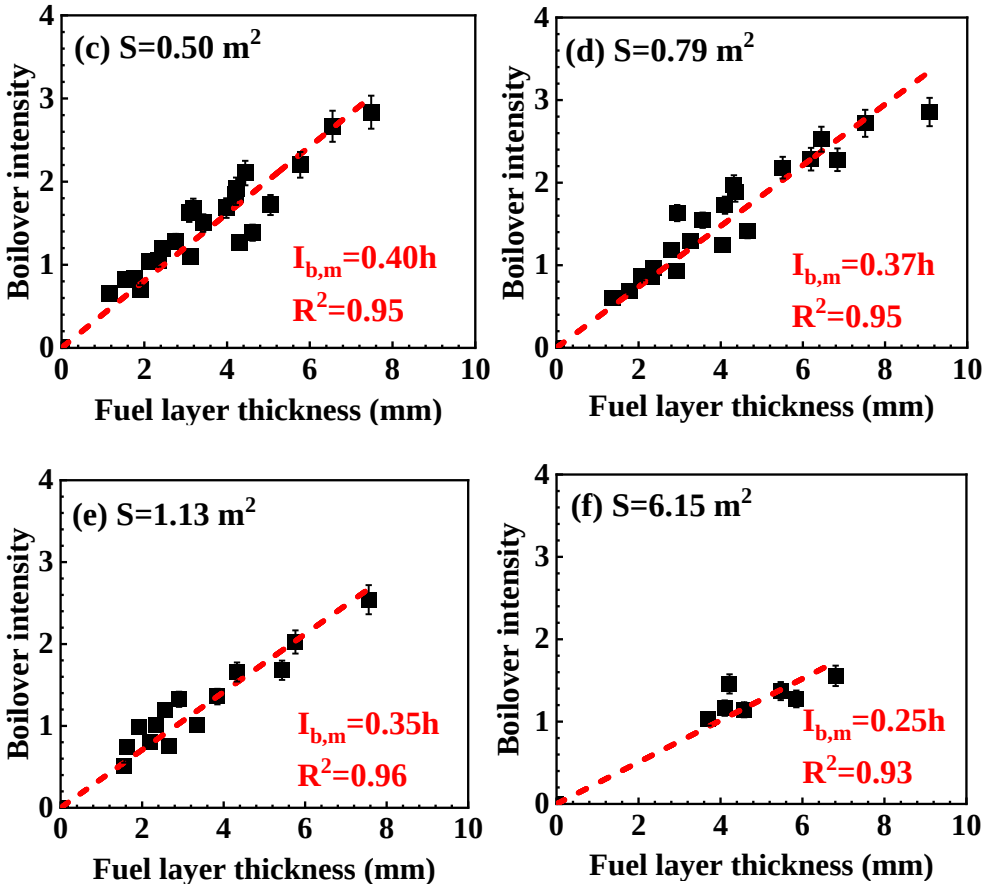

Fig. 5. The boilover intensity as a function of fuel thickness at boilover: a) S = 0.13 m^2; b) S = 0.28 m^2; c) S = 0.50 m^2; d) S = 0.79 m^2; e) S = 1.13 m^2; f) S = 6.15 m^2.

As mentioned in section 3.1, there was no steady burning stage for the burning with an initial fuel layer thickness of 3 mm, which makes it hard to determine the boilover intensity. This is mainly because for burning at only 3 mm fuel layer thickness, the fuel/water interface was very close to the fuel surface and was heated quickly. When the interface was heated to boiling temperature of water, a boiling layer was not formed at the fuel layer surface. Thus, the boilover intensity of tests with 3 mm fuel layer thickness is not analyzed. As shown in Fig. 5, the correlations of boilover intensity and fuel layer thickness under different pan areas are fitted and the

corresponding slopes $k^{'}$ are obtained ($k' = I_{b,m}/h$), respectively. It was found that the boilover intensity shows a linear dependency on the fuel layer thickness. The thicker the fuel layer when the boilover occurs, the greater the pressure at the fuel/water interface, resulting in more water vapor bubbles. As these bubbles burst through the fuel layer, more fuel droplets are carried out from the pan to the flame [7]. Meanwhile, the heating effect on water vapor bubbles is more obvious for thick fuel layer, leading to a more intense boilover.

3.2.2. Boilover intensity with pan area

The variation of boilover intensity coefficient $k^{'}$ with the pan area is analyzed in detail, as shown in Fig. 6(a).

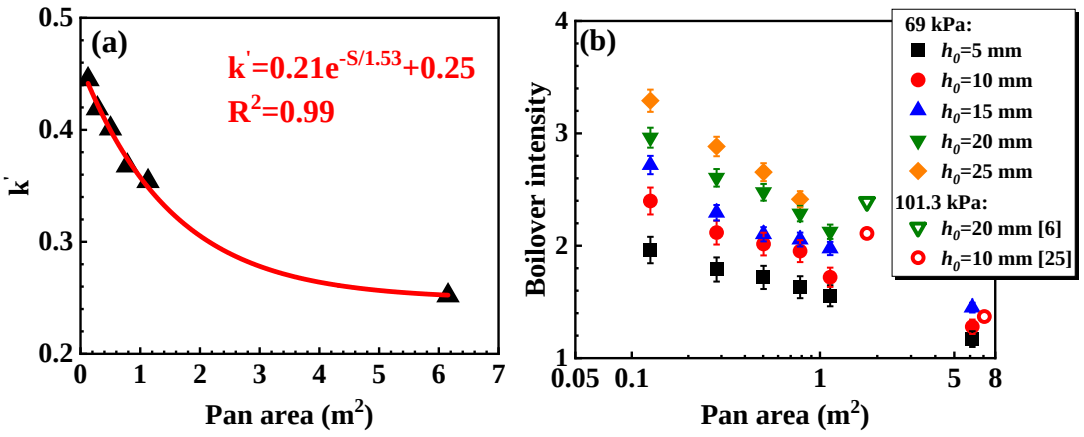

Fig. 6. a) The $k^{'}$ vs. pan area; b) The initial boilover intensity as a function of pan area based on flame height.

The corresponding correlation is also obtained by fitting as follows:

$$k' = 0.21e^{-S/1.53} + 0.25 \quad (12)$$

According to Fig. 6(a) and Eq. (12), the value of $k^{'}$ decreases in an exponential way with pan area. The decreasing range gradually reduces and the $k^{'}$ tends to a constant value. Fig. 6(b) presents the initial boilover intensity of thin-layer diesel burning

under different pan areas. It can be found that the boilover intensity decreases as the pan area increases with the same initial fuel layer thickness, which is consistent with the variation of $k^{'}$. This is because both the burning rate and the radiative heat flux reaching the fuel surface increase with increasing pan area. Then, the fuel consumption rate becomes faster and the residual fuel layer thickness is thinner when boilover occurs [26]. Meanwhile, the decreasing range of boilover intensity reduces gradually with pan area. Combined with the evolution of $k^{'}$, this clearly indicates that pool size has small effect on boilover intensity for large-scale burning. This is mainly due to that for pool fires with large pan area, the burning rate and flame height are relatively close, and the corresponding residual amount of fuel is almost the same when boilover occurs [27]. The previous experimental data of diesel boilover intensity under atmospheric pressure is also added in Fig. 6(b). The boilover intensity at sub-atmospheric pressure is lower than that under atmospheric pressure with the same pan area and fuel layer thickness. This can be attribute to the decrease in the boiling points of liquid fuel and water at sub-atmospheric pressure. When boilover occurs, there are fewer water vapor bubbles generated at the fuel/water interface and the heating effect of the fuel layer on the bubbles is also weakened [3].

3.2.3. Boilover intensity model

For thin-layer boilover fires, the key factors controlling the boilover intensity are [6, 7, 16, 26]: fuel boiling point T_{bf}, water boiling point T_{bw}, pan diameter D, initial fuel layer thickness h_0, fuel density ρ_f, acceleration of gravity g, air pressure P, dynamic viscosity μ, ambient temperature T_∞, air density ρ_∞, air specific heat at constant

pressure C_p, thermal conductivity k, thermal diffusivity α, mass burning rate $\dot{m}$, heat of combustion per unit fuel mass ΔH_c, i.e.

$$I_{b,a} = f(T_{bf}, T_{bw}, D, h_0, \rho_f, g, P, \mu, \rho_\infty, T_\infty, C_p, k, \alpha, \dot{m}, \Delta H_c) \tag{13}$$

Based on the dimensionless analysis, Eq. (13) can be expressed as:

$$I_{b,a} = f(\frac{T_{bf}}{T_\infty}, \frac{T_{bw}}{T_\infty}, \frac{h_0}{D}, \frac{\rho_f}{\rho_\infty}, \frac{gD^3}{\alpha^2}, \frac{PD^2}{\rho_\infty \alpha^2}, \frac{\mu}{\rho_\infty \alpha}, \frac{C_p T_\infty D^2}{\alpha^2}, \frac{kT_\infty D}{\rho_\infty \alpha^3}, \frac{\dot{m}D}{\rho_\infty \alpha}, \frac{\Delta H_c D^2}{\alpha^2}) \tag{14}$$

For pool fire, the heat release rate $\dot{Q}$ is expressed as follows [28]:

$$\dot{Q} = \frac{\pi \dot{m} D^2 \Delta H_c}{4} \tag{15}$$

Combined with Eq. (15), the Eq. (14) can be written as:

$$I_{b,a} = f(\frac{T_{bf}}{T_\infty}, \frac{T_{bw}}{T_\infty}, \frac{h_0}{D}, \frac{\dot{Q}}{\rho_\infty C_p T_\infty \sqrt{gD^5}}, \frac{P}{\rho_f g D}, \frac{C_p \mu}{k}) \tag{16}$$

The dimensionless heat release rate $\dot{Q}^*$ and Prandtl number Pr are introduced. The $\dot{Q}^*$ is closely associate with the heat release of boilover fires. The Prandtl number can reflect the influence of fluid characteristics on the heat transfer in the liquid layer.

$$\dot{Q}^* = \frac{\dot{Q}}{\rho_\infty C_p T_\infty \sqrt{gD^5}} \tag{17}$$

$$Pr = \frac{C_p \mu}{k} \tag{18}$$

Substituting Eq. (17-18) into Eq. (16), the correlation can be simplified as:

$$I_{b,a} = f(\frac{T_{bf}}{T_\infty}, \frac{T_{bw}}{T_\infty}, \frac{h_0}{D}, \dot{Q}^*, \frac{P}{\rho_f g D}, Pr) \tag{19}$$

$$I_{b,a} = f(\frac{\dot{Q}^* Pr h_0 P}{\rho_f g D^2}, \frac{T_{bf}}{T_\infty}, \frac{T_{bw}}{T_\infty}) \tag{20}$$

$$I_{b,a} = A(\frac{\dot{Q}^* h_0 P}{\rho_f g D^2})^{n_1} + B(\frac{T_{bf}}{T_\infty})^{n_2} + C(\frac{T_{bw}}{T_\infty})^{n_3} + E \tag{21}$$

where A, B, C, E, n_1, n_2 and n_3 are constants. For liquid fuel burning at stable ambient temperature and air pressure, $\frac{T_{bf}}{T_\infty}$ and $\frac{T_{bw}}{T_\infty}$ can be approximated as constant values. Meanwhile, the variation of pressure has little effect on ρ_f and g, which can be ignored. Eq. (21) can be further simplified as:

$$I_{b,a} = A'(\frac{\dot{Q}^* Pr \hbar_0 P}{D^2})^{n_1} + B' \quad (22)$$

As shown in Fig. 7, the best-fit correlation with the experimental data and the data from previous literatures is expressed as follows:

$$I_{b,a} = 0.02(\frac{\dot{Q}^* Pr \hbar_0 P}{D^2})^{0.40} + 1.12 \quad (23)$$

The R^2 is 0.92, and the predicted correlation is in good agreement with the work of Ferrero and Chatris et al with a maxim error less than 20 %. These indicates this model can well predict the boilover intensity under different conditions.

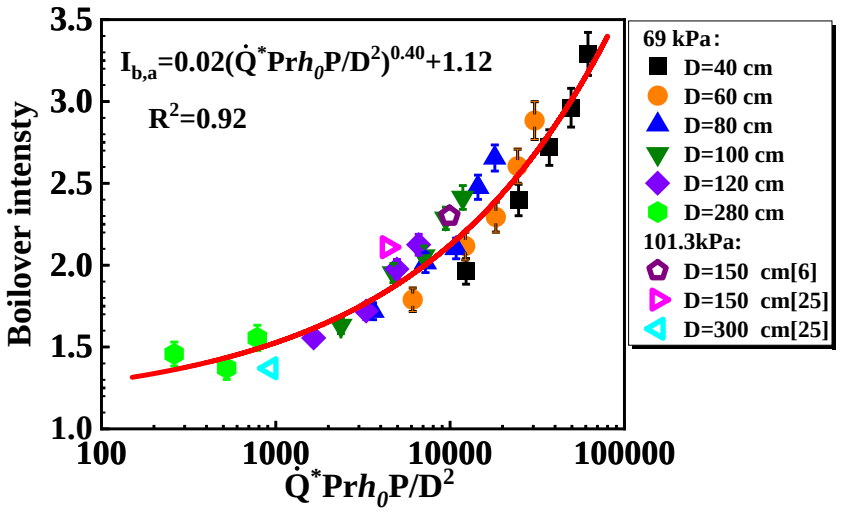

Fig. 7. The boilover intensity evolution as a function of $\frac{\dot{Q}^* Pr \hbar_0 P}{D^2}$.

3.3. Time to boilover onset

According to the findings in previous studies, the time to boilover onset in all tests is determined based on the fuel/water interface temperature, flame expansion and the variation of burning rate [4, 29]. Fig. 8 shows the time to boilover onset at different diameter and initial fuel layer thickness at sub-atmospheric pressure.

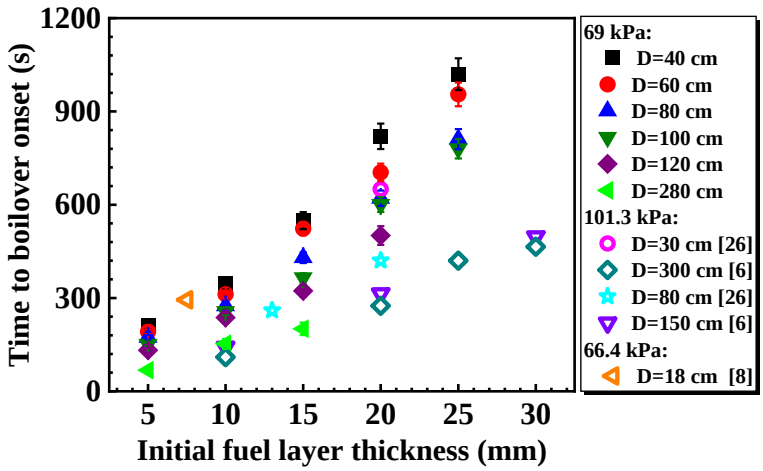

386

387 Fig. 8. The time to boilover onset evolution with initial fuel layer thickness.

388 As illustrated in Fig.8, the time to boilover onset shows a tendency to increase with
389 initial fuel layer thickness for the same diameter at sub-atmospheric pressure, which is
390 consistent with the variation of time to boilover onset under atmospheric pressure [26].
391 This is mainly because for thicker initial fuel layer thickness, it takes more time for
392 heat transfer to fuel/water interface, resulting in a longer time to reach the water
393 boiling point [6]. In addition, for the same initial fuel layer thickness, the time to
394 boilover onset decreases as the pan diameter increases. This is due to the mass
395 burning rate is faster and more heat is generated per unit of time with a larger
396 diameter. Thus, the fuel/water interface is heated to the water boiling temperature
397 faster [7].

398 Figure 8 also gives the experimental data of time to boilover onset under
399 atmospheric pressure in previous literatures. It can be found that the time to boilover
400 onset at sub-atmospheric pressure increases compared with that under atmospheric
401 pressure with the same diameter and initial fuel layer thickness. This is mainly
402 because the boiling point of liquid fuel becomes lower at sub-atmospheric pressure,

companied with the decrease of temperature at fuel surface. For example, the surface temperature of diesel pool fire is 320 ℃ at atmospheric pressure [6], while the value is 275 ℃ in this work. Thus, the downward heat transfer rate slows down, resulting in the delay of boilover onset time at sub-atmospheric pressure. Meanwhile, the mass burning rate decreases at sub-atmospheric pressure [30] and the effective heat transfer rate becomes slower, which lead to a decrease in the heating rate of fuel layer and interface.

Based on Eqs. (5-8), the following expression for the temperature distribution in the liquid layer can be obtained [31]:

$$\frac{T-T_\infty}{T_s-T_\infty} = \exp(\frac{r}{\alpha_{FW}}(y - y_s(t))) \tag{24}$$

When the temperature at fuel/water interface reaches the boiling point of water, the boilover occurs. In order to predict the time to boilover onset, the temperature at the fuel layer position y=0 is set as $T=T_{bw}$ when boilover occurs. The fuel surface is located at $y_s(t)=y_0-rt_b$. Thus, the Eq. (24) can be expressed as follows:

$$\frac{T_{bw}-T_\infty}{T_s-T_\infty} = \exp(\frac{r}{\alpha_{FW}}(rt_b - y_0)) \tag{25}$$

Eq. (25) can be simplified as:

$$t_b = \frac{1}{r}(\frac{\alpha_{FW}}{r}\ln\left(\frac{T_{bw}-T_\infty}{T_s-T_\infty}\right) + y_0) \tag{26}$$

Combined with Eq. (8), the above equation can be written as:

$$t_b = \frac{1}{r}\left(\frac{y_0}{\alpha_F}\left(\sqrt{\alpha_W} + \sqrt{\alpha_F}\right)^2 \ln\left(\frac{T_{bw}-T_\infty}{T_s-T_\infty}\right) + y_0\right) \tag{27}$$

The regression rate r is proved to be almost independent with initial fuel thickness for $y_0 > 5\ mm$ [16]. Thus, according to Eq. (9), it can be obtained that $r \propto \sqrt{D}$.

$$t_b \propto \frac{y_0}{\sqrt{D}}, \text{ that is, } t_b \propto \frac{h_0}{\sqrt{D}} \tag{28}$$

Therefore, the time to boilover onset can be expressed as:

$$t_b = k_1 \frac{h_0}{\sqrt{D}} + k_2 \tag{29}$$

In Fig. 9, the key parameters (k_1=27608; k_2=-14) are obtained by fitting the experimental data. Therefore, Eq. (30), which presents the correlation coefficient (R^2) of 0.97, can serve to predict the time to boilover onset at sub-atmospheric pressure (69 kPa):

$$t_b = 27608 \frac{h_0}{\sqrt{D}} - 14 \tag{30}$$

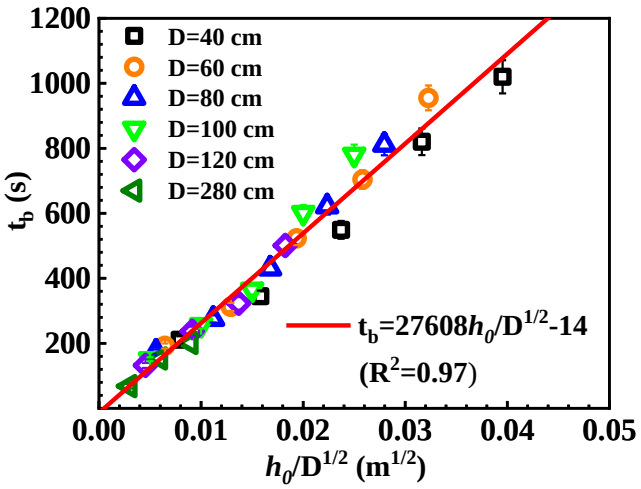

Fig. 9. The variation of time to boilover onset as function of h_0/D$^{1/2}$.

3.4. Boilover time interval

The phenomenon of continuous boilover occurs during the burning process of diesel thin-layer burning. The boilover time interval is closely related to the thermal hazard of boilover fires. Fig. 10 shows the variation of time interval between two adjacent boilovers at sub-atmospheric pressure.

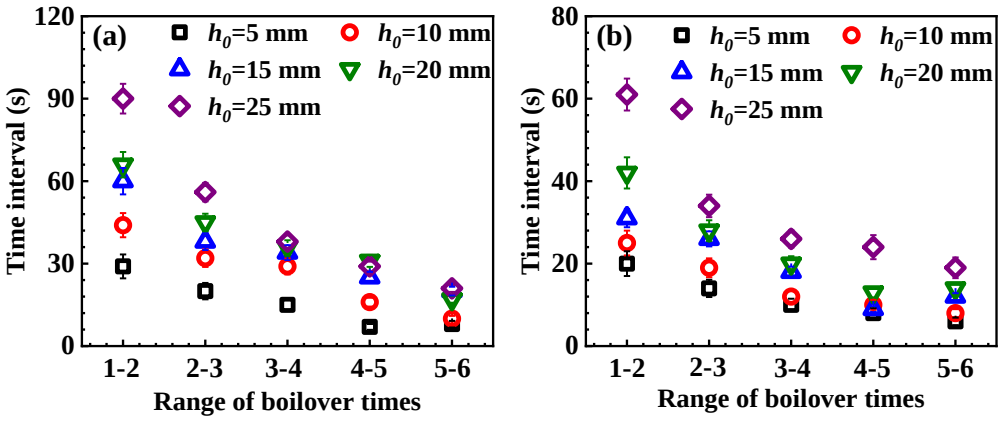

439

440 Fig. 10. The evolution of boilover time interval with range of boilover times:

441 a) D = 40 cm b) D = 80 cm.

442 In Fig. 10, the time interval between two adjacent boilovers decreases with the
443 number of boilover and the decreasing rate gradually slows down. Thus, the
444 uninterrupted boilovers occurs later in the continuous boilover stage, as observed in
445 the experiments. This is mainly because the residual fuel layer thickness decreases as
446 burning progresses. Thus, the vertical distance from the fuel/water interface to the
447 high-temperature fuel layer at fuel surface decreases with the increase of boilover
448 times [21], resulting in a stronger convection heat transfer between the fuel layer and
449 water layer. At the same time, the temperature at the fuel/water interface rises with the
450 number of boilover as shown in Fig. 11. The time required to heat the interface to the
451 boiling point of water is shortened. Moreover, it can also be observed in Fig. 10 that
452 the boilover time interval increases for the thicker fuel layer burning.

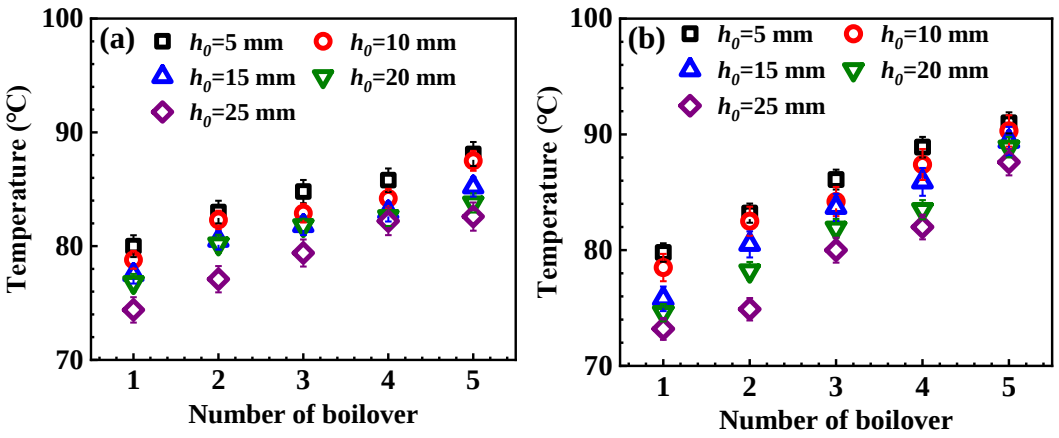

453

454 Fig. 11. The temperature of fuel/water interface vs. boilover times

455 a) D = 40 cm b) D = 80 cm.

456 It can be seen in Fig.10 that the boilover time interval decreases with the increasing
457 pan diameter compared with Fig.10(a) and Fig.10(b). This is mainly because as the
458 pan diameter increases, both the mass burning rate and the surface heat flux increase.
459 Then, the liquid layer is heated faster and the fuel/water interface reaches the boiling
460 temperature of water again sooner after boilover.

461 **4. Conclusions**

462 Large-scale boilover fire experiments with a thin-layer of diesel on water were
463 performed at sub-atmospheric pressure. The burning process, boilover intensity, time
464 to boilover onset and boilover time interval were analyzed and the corresponding
465 models were established. The influence of the initial fuel layer thickness and pan
466 diameter on these key parameters were investigated in detail. The main findings are
467 drawn as follows:

468 (1) Based on the variation of flame shape, the burning process of diesel boilover at
469 sub-atmospheric pressure can be divided into four typical stages: initial development
470 stage, steady burning stage, continuous boilover stage, and decay stage. Meanwhile,

there is no steady burning stage for boilover fires with a small fuel layer thickness, in which the value is 3 mm in the current study. For the continuous boilover stage, the flame height increases significantly at initial boilover. The flame height decreases gradually and the boilover time interval is shortened for the subsequent multiple boilovers. In addition, weak burning occurs and the temperature of fuel layer decreases after boilover, which is attributed to the destruction of the boiling layer.

(2) The initial boilover intensity shows a linearly dependency on fuel layer thickness, and the increasing range decreases with pan area. Meanwhile, the pan area has a limited effect on boilover intensity for large-scale burning. Moreover, the boilover intensity at sub-atmospheric pressure is lower than that under atmospheric pressure with the same other conditions. Based on the dimensionless analysis, a predictive expression for boilover intensity was established ($I_{b,a} = 0.02(\frac{\dot{Q}^* Pr \hbar_0 P}{D^2})^{0.40} + 1.12$).

(3) The time to boilover onset increases positively with the initial fuel layer thickness and negatively with the pan diameter, which is consistent with the findings under atmospheric pressure. The time to boilover onset at sub-atmospheric pressure is delayed compared with that under atmospheric pressure. Based on the one-dimensional, two-layer conduction model, a predictive expression for the time to boilover onset at sub-atmospheric pressure (69 kPa) was developed ($t_b = 27608 \frac{h_0}{\sqrt{D}} - 14$).

(4) The boilover time interval at sub-atmospheric pressure decreases as the number of boilover increases and the decreasing range decreases gradually, followed by close

to uninterrupted boilovers. Meanwhile, the boilover time interval increases with initial fuel thickness and decreases with burning scale.

Finally, it should be noted that present work mainly using diesel studied the evolution of continuous boilover behaviors at a certain sub-atmospheric pressure. In the future, more experiments will be performed using different liquid fuels and pressure conditions for further validation of the models proposed in this work.

Acknowledgements

This work was sponsored by the National Key R&D Program of China (2021YFB3201902), the Key Research and Development Program of National Fire and Rescue Administration (No. 2022XFZD04), the European Union's Horizon 2020 research and innovation program (No. 952395) and the Fundamental Research Funds for the Central Universities (No. 2020QN05).

Reference

[1] Wang Y. Oil Tank Fire in Kuche County, Aksu, Xinjiang. China Fire 2014;16:12-13.

[2] Hu L, Tang F, Wang Q, Qiu Z. Burning characteristics of conduction-controlled rectangular hydrocarbon pool fires in a reduced pressure atmosphere at high altitude in Tibet. Fuel 2013;111:298-304.

[3] Ding C. Experimental research on the flashpoint-boiling point of flammable liquid and their applications under low pressure. Hefei: University of Science and Technology of China; 2016. PhD Thesis.

[4] Fan WC, Hua JS, Liao GX. Experimental study on the premonitory phenomena of

boilover in liquid pool fires supported on water. J Loss Prevent Proc 1995;8(4):221-227.

[5] Koseki H, Kokkala M, Mulholland GW. Experimental study of boilover in crude oil fires. Fire Saf Sci 2006; 865-874.

[6] Ferrero F, Muñoz M, Kozanoglu B, Casal J, Arnaldos J. Experimental study of thin-layer boilover in large-scale pool fires. J Hazard Mater 2006;137(3):1293-1302.

[7] Kong D, Liu P, Zhang J, Fan M, Tao C. Small scale experiment study on the characteristics of boilover. J Loss Prevent Proc 2017, 48:101-110.

[8] Chen Q, Liu X, Wang X, Zhao J, Zhou T, Ding C, et al. Experimental study of liquid fuel boilover behavior in normal and low pressures. Fire Mater 2018;42(7):843-858.

[9] Lin X. Experiment on characteristics of small-scale thin layer boilover[D]. Hefei: University of Science and Technology of China; 2017. PhD Thesis.

[10] Arai M, Saito K, Altenkirch R A. A study of boilover in liquid pool fires supported on water part I: effects of a water sublayer on pool fires. Combust Sci Technol 1990; 71(1-3):25-40.

[11] Broeckmann B, Schecker H G. Heat transfer mechanisms and boilover in burning oil-water systems. J Loss Prevent Proc 1995;8(3):137-147.

[12] E. Twardus, T. Brzustowski. The burning of crude oil spilled on water Arch. Combust 1981;1:1–2.

[13] Brzustowski TA, Twardus EM. A Study of the Burning of a Slick of Crude Oil on Water. Symposium (International) on Combustion. Elsevier 1982;19(1):847-854.

537 [14] Alramadhan M A, Arpaci V S, Selamet A. Radiation affected liquid fuel burning
538 on water. Combust Sci Technol 1990;72(4-6):233-253.
539 [15] Inamura T, Saito K, Tagavi KA. A study of boilover in liquid pool fires supported
540 on water. Part II: effects of in-depth radiation absorption. Combust Sci Technol 1992;
541 86(1-6):105-119.
542 [16] Garo J P, Vantelon J P, Gandhi S, Torero, JL. Determination of the thermal
543 efficiency of pre-boilover burning of a slick of oil on water. Spill Sci Technol Bull
544 1999;5(2):141-151.
545 [17] Zhao J, Zhang Q, Zhang X, Zhang J, Yang R, Lu Y. Experimental study and
546 thermal hazard analysis of large-scale n-heptane pool fires under sub-atmospheric
547 pressure. Process Saf Environ 2022;166: 279-289.
548 [18] Drysdale D. An introduction to fire dynamics. John wiley & sons 2011.
549 [19] Beyler C L. Fire hazard calculations for large, open hydrocarbon fires. SFPE
550 handbook of fire protection engineering 2016;2591-2663.
551 [20] van Gelderen L, Brogaard NL, Sørensen MX, Fritt-Rasmussen J, Rangwala AS,
552 Jomaas G. Importance of the slick thickness for effective in-situ burning of crude oil.
553 Fire Saf J 2015;78:1-9.
554 [21] Zhao J, Zhang J, Chen C, Huang H, Yang R. Experimental investigation on the
555 burning behaviors of thin-layer transformer oil on a water layer. Process Saf Environ
556 2020;139:89-97.
557 [22] Vali A, Nobes D S, Kostiuk L W. Transport phenomena within the liquid phase of
558 a laboratory-scale circular methanol pool fire. Combust Flame

559 2014;161(4):1076-1084.
560 [23] Hu L, Wang Q, Delichatsios M, Tang F, Zhang X, Lu S. Flame height and lift-off
561 of turbulent buoyant jet diffusion flames in a reduced pressure atmosphere. Fuel
562 2013;109:234-240.
563 [24] Tao C, Liu B, Dou Y, Qian Y, Zhang Y, Meng S. The experimental study of flame
564 height and lift-off height of propane diffusion flames diluted by carbon dioxide. Fuel
565 2021;290: 119958.
566 [25] Chatris JM, Planas E, Arnaldos J, Casal J. Effects of thin-layer boilover on
567 hydrocarbon pool fires. Combust Sci Technol 2001;171(1):141-161.
568 [26] Garo JP, Vantelon JP, Koseki H. Thin-layer boilover: Prediction of its onset and
569 intensity. Combust Sci Technol 2006;178(7):1217-1235.
570 [27] Babrauskas V. Estimating large pool fire burning rates. Fire Technol
571 1983;19:251-261.
572 [28] Heskestad G. On Q* and the dynamics of turbulent diffusion flames. Fire Saf J
573 1998;30(3):215-227.
574 [29] Hua JS, Fan WC, Liao GX. Study and prediction of boilover in liquid pool fires
575 with a water sublayer using micro-explosion noise phenomena. Fire Saf J
576 1998;30(3):269-291.
577 [30] Wieser D, Jauch P, Willi U. The influence of high altitude on fire detector test
578 fires. Fire Saf J, 1997;29(2-3):195-204.
579 [31] Garo JP, Vantelon JP, Fernandez-Pello AC. Boilover burning of oil spilled on
580 water. Symp (Int) on Combust 1994;25(1):1481-1488.